A dynamical inflaton coupled to strongly interacting matter

Christian Ecker,[1] Elias Kiritsis,[2,3] and Wilke van der Schee[4,5]

[1]*Institut für Theoretische Physik, Goethe Universität, Max-von-Laue-Str. 1, 60438 Frankfurt am Main, Germany*
[2]*Université Paris Cité, CNRS, Astroparticule et Cosmologie, F-75013 Paris, France*
[3]*Institute for Theoretical and Computational Physics, Department of Physics, P.O. Box 2208,University of Crete, 70013, Heraklion, Greece*
[4]*Theoretical Physics Department, CERN, CH-1211 Genève 23, Switzerland*
[5]*Institute for Theoretical Physics, Utrecht University, 3584 CC Utrecht, The Netherlands*

(Dated: May 22, 2023)

I. SUPPLEMENTAL MATERIAL

A. Variational Principle with Mixed Boundary Conditions

In this appendix we review the variational principle in holography with dynamical boundary conditions for the source fields [1–3]. We will restrict to the case relevant to this work, namely Einstein-dilaton gravity with dynamical boundary conditions for the metric and the scalar field governed by four-dimensional Einstein-inflaton equations of motion.

In the supergravity limit, the gauge/gravity duality allows to express the partition function of a strongly coupled quantum field theory (QFT) as a path integral of a higher dimensional gravity action

$$Z_{\rm QFT}[\gamma,\phi] = \int [\mathcal{D}g]_\gamma [\mathcal{D}\Phi]_\phi e^{-S_{\rm hol}}\,, \tag{1}$$

where γ_{ij} and ϕ denote the background geometry of the dual QFT and the inflaton field on the boundary, while $\int[\mathcal{D}g]_\gamma[\mathcal{D}\Phi]_\phi$ means integration over all bulk geometries and scalar fields with fixed boundary conditions γ_{ij} and ϕ, respectively. Promoting γ_{ij} and ϕ to dynamical fields allows one to define an induced gravity partition function as a path integral over all boundary fields

$$\begin{aligned} Z_{\rm ind} &= \int \mathcal{D}\gamma\mathcal{D}\phi Z_{\rm QFT}[\gamma,\phi] \\ &= \int \mathcal{D}\gamma\mathcal{D}\phi \int [\mathcal{D}g]_\gamma [\mathcal{D}\Phi]_\phi e^{-S_{\rm hol}} \\ &= \int \mathcal{D}g\mathcal{D}\Phi e^{-S_{\rm hol}}\,. \end{aligned} \tag{2}$$

Because the boundary fields are dynamical, the variations of the action result, in addition to the bulk equations of motion, also in some non-trivial boundary contributions

$$\begin{aligned} \delta_g S_{\rm hol} &= \int_{\mathcal{M}} {\rm d}x^5 \sqrt{-g}\, {\rm EOM}^{\rm (g)}_{\rm bulk}\, \delta g^{\mu\nu} \\ &\quad + \int_{\partial\mathcal{M}} {\rm d}x^4 \sqrt{-\gamma} \frac{1}{2} \langle T^{\rm QFT}_{ij} \rangle \delta\gamma^{ij}\,, \end{aligned} \tag{3}$$

$$\begin{aligned} \delta_\Phi S_{\rm hol} &= \int {\rm d}x^5 \sqrt{-g}\, {\rm EOM}^{(\Phi)}_{\rm bulk}\, \delta\Phi^{\mu\nu} \\ &\quad + \int_{\partial\mathcal{M}} {\rm d}x^4 \sqrt{-\gamma} \langle \mathcal{O} \rangle \delta\phi\,. \end{aligned} \tag{4}$$

Since $S_{\rm hol}$ includes the counter terms, whose explicit form is derived in the next section, the boundary contributions can be identified with the expectation values of the renormalized holographic stress tensor $\langle T^{\rm QFT}_{ij}\rangle$ and the scalar field operator $\langle\mathcal{O}\rangle$ of the boundary theory.

There are different ways to make the actions (3) and (4) stationary [1]. The simplest option is to impose Dirichlet boundary conditions on $g_{\mu\nu}$ and Φ, i.e., demanding $\delta\gamma_{ij} = 0$ and $\delta\phi = 0$, which makes the boundary geometry and the inflaton field static. Another option is to impose Neuman boundary conditions, which is demanding $\langle T^{\rm QFT}_{ij}\rangle = \langle\mathcal{O}\rangle = 0$. In this case γ_{ij} and ϕ can remain dynamical and the bulk geometry is fixed to empty AdS$_5$. Combinations of these two options are of course also possible. Finally, the most general possibility is to impose mixed boundary conditions, that is to demand $\frac{1}{2}\langle T^{\rm QFT}_{ij}\rangle + \frac{\delta S_{\rm bdry,\gamma}}{\delta\gamma^{ij}} = 0$ and $\langle\mathcal{O}\rangle + \frac{\delta S_{\rm bdry,\phi}}{\delta\phi} = 0$ for some functionals of the boundary metric $S_{\rm bdry,\gamma}$ and the scalar field $S_{\rm bdry,\phi}$ that can be added to the bulk action. In this work we choose these boundary functionals to be given by the Einstein-Hilbert plus inflaton action $S_{\rm EH+inf}[\phi,\gamma_{ij}]$ and the interaction term $S_{\rm int}[\phi,\gamma_{ij}]$.

B. Holographic Renormalization

In this appendix we derive the explicit form of the renormalized expectation values of the holographic energy momentum tensor and the scalar field operator [4–6]. In the following we assume Fefferman–Graham (FG) gauge

$$ds^2 = L^2 \frac{{\rm d}\rho^2}{4\rho^2} + \bar{g}_{ij}(\rho,x){\rm d}x^i{\rm d}x^j\,, \tag{5}$$

where the boundary is located at $\rho = 0$ and is parametrized by the coordinates x^i with $i = 0,\ldots,3$ and L denotes the Anti-de Sitter length scale which we set to unity. Near the boundary the metric and the scalar field take the form

$$\begin{aligned} \bar{g}_{ij}(\rho,x) &= \frac{1}{\rho}\Big[\gamma_{ij}(x) + \rho\,\gamma_{(2)ij}(x) + \rho^2\gamma_{(4)ij}(x) \\ &\quad + \rho^2 \log\rho\, h_{(4)ij}(x) + O(\rho^3)\Big]\,, \end{aligned} \tag{6}$$

$$\begin{aligned} \Phi(\rho,x) &= \rho^{1/2}\Big[\Phi_{(0)}(x) + \rho\,\Phi_{(2)}(x) \\ &\quad + \rho\,\log\rho\,\psi_{(2)}(x) + O(\rho^2)\Big]\,. \end{aligned} \tag{7}$$

The first term $\gamma_{ij}(x)$ in the expansion of the metric is the boundary metric and the term $\Phi_{(0)}(x)$ plays the role of the inflaton field in the boundary theory. The Klein–Gordon equation for the scalar field fixes the logarithmic coefficient $\psi_{(2)}$ in terms of γ_{ij} and $\Phi_{(0)}$ as

$$\psi_{(2)} = \frac{1}{4}\left(\nabla^2\Phi_{(0)} - \frac{1}{6}\Phi_{(0)}R\right). \tag{8}$$

At leading order Einstein's equations determine

$$\gamma_{(2)ij} = -\frac{1}{2}\left(R_{ij} - \frac{1}{6}R\,\gamma_{ij}\right) - \frac{\Phi_{(0)}^2}{3}\gamma_{ij}. \tag{9}$$

The logarithmic part at sub-leading order fixes

$$\begin{aligned} h_{(4)ij} = h^{\text{grav}}_{(4)ij} &- \frac{1}{12}R_{ij}\Phi_{(0)}^2 - \frac{1}{3}\nabla_i\Phi_{(0)}\nabla_j\Phi_{(0)} \\ &+ \frac{1}{12}\nabla_i\Phi_{(0)}\nabla^i\Phi_{(0)}\,\gamma_{ij} + \frac{1}{6}\Phi_{(0)}\nabla_i\nabla_j\Phi_{(0)} \\ &+ \frac{1}{12}\Phi_{(0)}\,\Box_\gamma\,\Phi_{(0)}\,\gamma_{ij}, \end{aligned} \tag{10}$$

where the pure gravitational part is given by

$$\begin{aligned} h^{\text{grav}}_{(4)ij} = \frac{1}{8}R_{ikjl}R^{kl} - \frac{1}{48}\nabla_i\nabla_j R + \frac{1}{16}\nabla^2 R_{ij} - \frac{1}{24}RR_{ij} \\ + \left(\frac{1}{96}R^2 - \frac{1}{96}\nabla^2 R - \frac{1}{32}R_{kl}R^{kl}\right)\gamma_{ij}. \end{aligned} \tag{11}$$

The expectation values of the holographic energy momentum tensor and the scalar field operator follow from variations of the renormalized action of the holographic model

$$S_{\text{hol}} = S_{\text{bulk}} + S_{\text{GHY}} + S_{\text{ct}}. \tag{12}$$

The bare bulk action S_{bulk} is defined in Eq. (5) of the main text and the second term is the Gibbons–Hawking–York (GHY) boundary term

$$S_{\text{GHY}} = \frac{1}{\kappa_5}\int \mathrm{d}^4x\sqrt{-\gamma}K, \tag{13}$$

where $K = \gamma^{ij}K_{ij} = \gamma^{ij}\nabla_i n_j$ denotes the trace of the extrinsic curvature of a four-dimensional slice of the bulk geometry near the boundary. The last contribution in (12) is a counter term that is defined on a constant-ρ hypersurface near the boundary, which is necessary to render the on-shell action S_{hol} finite in the limit $\rho \to 0$

$$\begin{aligned} S_{\text{ct}} = \frac{1}{\kappa_5}\int \mathrm{d}^4x\sqrt{-\gamma}\Bigg[\left(-\frac{1}{8}R - \frac{3}{2} - \frac{1}{2}\Phi_{(0)}^2\right) \\ + \frac{1}{2}(\log\rho)\,\mathcal{A} + \left(\alpha\mathcal{A} + \beta\Phi_{(0)}^4\right)\Bigg], \end{aligned} \tag{14}$$

where the constants α and β parametrize the residual renomalization-scheme ambiguity of the model. The holographic conformal anomaly [7, 8] $\mathcal{A} = \mathcal{A}_g + \mathcal{A}_\phi$ consists of a gravitational part due to the curved boundary geometry

$$\mathcal{A}_g = \frac{1}{16}(R^{ij}R_{ij} - \frac{1}{3}R^2), \tag{15}$$

and a part due to scalar matter

$$\mathcal{A}_{\Phi_{(0)}} = -\frac{1}{2}\left(\partial_i\Phi_{(0)}\partial^i\Phi_{(0)} + \frac{1}{6}R\Phi_{(0)}^2\right). \tag{16}$$

All this together results in the following expression for the holographic stress tensor

$$\begin{aligned} \langle T^{\text{QFT}}_{ij}\rangle &= \frac{2}{\sqrt{-\gamma}}\frac{\delta S_{\text{hol}}}{\delta\gamma^{ij}} \\ &= \frac{2}{\kappa_5}\Bigg\{\gamma_{(4)ij} + \frac{1}{8}\left[\text{Tr}\gamma_{(2)}^2 - (\text{Tr}\gamma_{(2)})^2\right]\gamma_{ij} \\ &- \frac{1}{2}\gamma_{(2)}^2 + \frac{1}{4}\gamma_{(2)ij}\text{Tr}\gamma_{(2)} + \frac{1}{2}\partial_i\Phi_{(0)}\partial_j\Phi_{(0)} \\ &+ \left(\Phi_{(0)}\Phi_{(2)} - \frac{1}{2}\Phi_{(0)}\psi_{(2)} - \frac{1}{4}\partial_k\Phi_{(0)}\partial^k\Phi_{(0)}\right)\gamma_{ij} \\ &+ \alpha\left(\mathcal{T}^\gamma_{ij} + \mathcal{T}^\phi_{ij}\right) + \left(\frac{1}{18} + \beta\right)\Phi_{(0)}^4\gamma_{ij}\Bigg\}. \end{aligned} \tag{17}$$

The anomalous contributions to the stress tensor are given by

$$\mathcal{T}^g_{ij} = 2h_{(4)ij}, \tag{18}$$

$$\begin{aligned} \mathcal{T}^\phi_{ij} = &-\frac{1}{2}\Phi_{(0)}^2R_{ij} - \frac{2}{3}\nabla_i\Phi_{(0)}\nabla_j\Phi_{(0)} + \frac{1}{6}\gamma^{kl}\nabla_k\nabla_l\Phi_{(0)}\gamma_{ij} \\ &+ \frac{1}{3}\Phi_{(0)}\nabla_i\nabla_j\Phi_{(0)} + \frac{1}{6}\Phi_{(0)}\Box\Phi_{(0)}\gamma_{ij} \\ &- \frac{1}{2}\gamma_{ij}\left(\Phi_{(0)}\Box\Phi_{(0)} - \frac{1}{6}R\Phi_{(0)}^2\right). \end{aligned} \tag{19}$$

The expectation value of the scalar operator in the field theory is then given by

$$\begin{aligned} \langle\mathcal{O}\rangle &= \frac{1}{\sqrt{-\gamma}}\frac{\delta S_{\text{hol}}}{\delta\Phi_{(0)}} \\ &= \frac{2}{\kappa_5}\left[(1-4\alpha)\psi_{(2)} - 2\Phi_{(2)} - 4\beta\Phi_{(0)}^3\right]. \end{aligned} \tag{20}$$

The holographic stress tensor satisfies anomaly-corrected Ward identities

$$\nabla^i\langle T^{\text{QFT}}_{ij}\rangle = -\langle\mathcal{O}\rangle\nabla_j\Phi_{(0)}, \tag{21}$$

$$\gamma^{ij}\langle T^{\text{QFT}}_{ij}\rangle = -\Phi_{(0)}\langle\mathcal{O}\rangle + \frac{1}{\kappa_5}\left(\mathcal{A}_g + \mathcal{A}_{\Phi_{(0)}}\right). \tag{22}$$

The inflaton field in the main text $\phi = \Phi_{(0)}/\lambda$ is related to the source of the scalar operator $\Phi_{(0)}$ via the coupling constant λ and all QFT expectation values are given in units of the bulk gravitational coupling

$$\begin{aligned} \mathcal{T}^{\text{QFT}}_{ij} &= \kappa_5\langle T^{\text{QFT}}_{ij}\rangle \\ &= \text{diag}\left(\mathcal{E}_{\text{QFT}}, \mathcal{P}_{\text{QFT}}, \mathcal{P}_{\text{QFT}}, \mathcal{P}_{\text{QFT}}\right), \end{aligned} \tag{23}$$

$$\mathcal{O}_{\text{QFT}} = \kappa_5\langle\mathcal{O}\rangle. \tag{24}$$

Finally, in our setup with dynamical boundary equations, α and β renormalize the bare gravitational coupling and the cosmological constant in the boundary theory [9]

$$\frac{1}{\kappa_4} = \frac{1}{\kappa_{4,\text{bare}}} + \frac{\alpha}{96\,\kappa_5}, \tag{25}$$

$$\frac{\Lambda_4}{\kappa_4} = \frac{\Lambda_{4,\text{bare}}}{\kappa_4} - \frac{\beta}{1024\,\pi}. \tag{26}$$

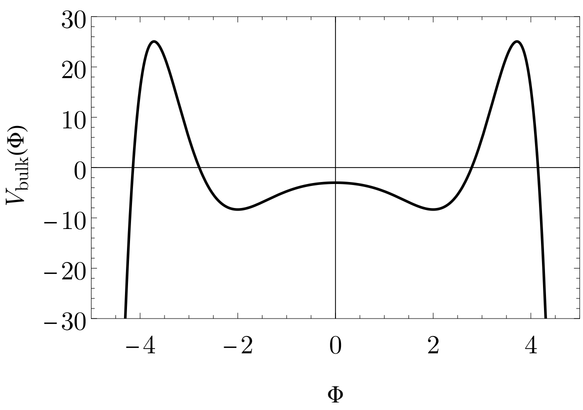

FIG. 1. Scalar field potential of the holographic model.

We fix $\alpha = 0$ and $\beta = \frac{1}{16}$, because this choice leads to a supersymmetric renormalisation scheme in which the full boundary stress tensor vanishes identically if the boundary metric is flat.

C. Properties of the holographic QFT

Here we review some basic properties of the holographic QFT used in this work (see also [10]). This theory has a relevant scalar operator that is dual to a bulk scalar field Φ. For convenience, we repeat here the corresponding Einstein-dilaton type bulk action

$$S_{\rm bulk} = \frac{2}{\kappa_5}\int {\rm d}^5x\sqrt{-g}\left(\frac{1}{4}\mathcal{R} - \frac{1}{2}(\partial\Phi)^2 - V_{\rm bulk}(\Phi)\right), \tag{27}$$

where κ_5 denotes the bulk gravitational coupling, $\mathcal{R}$ is the Ricci scalar associated to the bulk metric $g_{\mu\nu}$ and Φ is the bulk scalar field with potential

$$V_{\rm bulk}(\Phi) = \frac{1}{L^2}\left(-3 - \frac{3\Phi^2}{2} - \frac{\Phi^4}{3} + \frac{11\Phi^6}{96} - \frac{\Phi^8}{192}\right). \tag{28}$$

The bulk potential $V_{\rm bulk}(\Phi)$ has several extrema and is shown in Fig. 1. The most interesting for us is the maximum at $\Phi = 0$, which corresponds to an UV fixed point, or a $\rm CFT_{UV}$. On the two sides of this maximum are two symmetric minima at $\Phi = \pm 2$ that correspond to two copies of an IR conformal theory $\rm CFT_{IR}$. As the potential has a $\Phi \to -\Phi$ symmetry, the two minima correspond to the same $\rm CFT_{IR}$. Around the maximum, the dimension of the relevant scalar operator is $\Delta_{\rm UV} = 3$, while at the minima the dimension of the same scalar operator is $\Delta_{\rm IR} = 25/6$. The relevant coupling in the $\rm CFT_{UV}$ has mass dimension one, and is therefore like a fermion mass scale. Our QFT is a RG flow between $\rm CFT_{UV}$ and $\rm CFT_{IR}$ that is driven by the source of the scalar operator with mass scale m. Moreover, the QFT has the symmetry $m \to -m$. This QFT is therefore massless in the IR, with the massless (and strongly coupled) degrees of freedom being those of $\rm CFT_{\it IR}$. Moreover, although the QFT is strongly coupled at all scales, it is a non-confining QFT.

The thermodynamic and transport properties of the model were analyzed in [11]. At $T > 0$ the theory is entering the black-hole phase and remains in it, all the way to $T \to \infty$. In Fig. 2 (reproduced from [10]) we show from left to right the dimensionless entropy ratio s/T^3 as a function of the (dimensionless) temperature, the ratio $3\mathcal{P}/\mathcal{E}$ of the pressure to the energy density and ratio of the bulk viscosity to the entropy density, ζ/s, as function of energy density. All these quantities asymptote to their conformal values at small and large temperatures or energy densities.

Finally, we comment here on the evolution of the QFT when it is coupled to the inflaton. The inflaton field is by construction proportional to the mass scale of the QFT. When the inflaton slow-rolls in the potential on the left side of Fig. 2 in the main text, the mass scale of the QFT starts at large negative values and slowly increases towards zero. This represents an inverse RG flow that is driven by the cosmological evolution of the inflaton. Once the inflaton settles at the minimum of the potentials at $\Phi = 0$, the mass scale becomes zero and leaves the QFT at its UV limit, namely $\rm CFT_{\it UV}$.

D. Solving the Bulk Model Numerically

The action in Eq. (1) of the main text results in a coupled set of equations of motion for the bulk that are the five-dimensional Einstein–Klein–Gordon equations

$$\mathcal{R}_{\mu\nu} - \frac{1}{2}\mathcal{R}\, g_{\mu\nu} = 2\partial_\mu\Phi\partial_\nu\Phi - g_{\mu\nu}\left(2V_{\rm bulk} + (\partial\Phi)^2\right) \tag{29}$$

$$\Box_g\Phi = \frac{\partial V_{\rm bulk}}{\partial\Phi}\,. \tag{30}$$

The method we use to solve the corresponding initial value problem for fixed boundary conditions was first presented in [12] for pure gravity and further reviewed in [13, 14]. For the case of dynamical boundary conditions as studied here, the method was first extended numerically in [9]. Here we give a summary of this method.

For the numerical treatment of the initial value problem it is convenient to use generalized Eddington–Finkelstein (EF) coordinates rather than FG gauge to parametrize the bulk geometry and the scalar field

$$ {\rm d}s^2_{\rm bulk} = g_{\mu\nu}{\rm d}x^\mu {\rm d}x^\nu \tag{31}$$

$$ = -A(r,t){\rm d}t^2 + 2{\rm d}r{\rm d}t + S(r,t)^2{\rm d}\vec{x}^2\,, \tag{32}$$

$$\Phi = \Phi(r,t)\,, \tag{33}$$

where the asymptotic boundary is located at $r = \infty$. In this gauge the coupled set of Einstein and scalar field equations

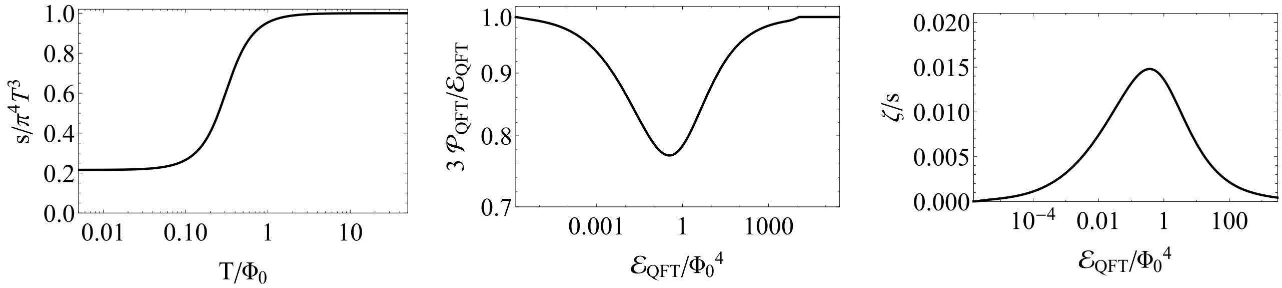

FIG. 2. We show the thermodynamical entropy density (left), pressure (middle) and bulk viscosity (right) as a function of temperature or energy density. This figure is reproduced from [10] (see also [11]).

result in the following nested set of ODEs

$$S'' = -\frac{2}{3}S\,(\Phi')^2\,, \tag{34}$$

$$\dot{S}' = -\frac{2\dot{S}S'}{S} - \frac{2SV}{3}\,, \tag{35}$$

$$\dot{\Phi}' = \frac{V'}{2} - \frac{3\dot{S}\Phi'}{2S} - \frac{3S'\dot{\Phi}}{2S}\,, \tag{36}$$

$$A'' = \frac{12\dot{S}S'}{S^2} + \frac{4V}{3} - 4\dot{\Phi}\Phi'\,, \tag{37}$$

$$\ddot{S} = \frac{\dot{S}A'}{2} - \frac{2S\dot{\Phi}^2}{3}\,, \tag{38}$$

where a prime denotes a radial derivative, $f' \equiv \partial_r f$, and an overdot is short-hand for the modified derivative $\dot{f} \equiv \partial_t f + \frac{1}{2}A\partial_r f$. The beauty of the scheme of this so-called characteristic formulation is that specifying $\Phi(z)$ leads to $\partial_t\Phi(z)$ through this nested set of ODEs, which is much simpler than the typical PDE system encountered in numerical relativity. We solve the initial value problem using the procedure explained in [10] imposing the Friedmann–Lemaître–Robertson–Walker metric

$$\mathrm{d}s^2 = \gamma_{ij}\mathrm{d}x^i\mathrm{d}x^j = -\mathrm{d}t^2 + a(t)^2\mathrm{d}\vec{x}^2\,, \tag{39}$$

which leads to the boundary condition $S(r) = r\,a(t) + \mathcal{O}(r^0)$ for Eq. (34). The boundary conditions for Eq. (35) and Eq. (36) is fixed by demanding regularity near the boundary, while for Eq. 37 they are fixed by the energy density $\mathcal{E}$. The energy density is evolved by using conservation of the stress-energy tensor or alternatively by using Eq. (38).

In practice it is difficult to solve these equations directly. For numerical efficiency it is better to switch coordinates to $z = 1/r$ and to perform a near-boundary (NB) expansion of both the equations and the functions S, A and Φ. One then redefines $\Phi(r) \equiv \Phi_{NB}(r) + r^{-3}\tilde{\Phi}(r)$ with $\Phi_{NB}(r)$ containing near-boundary terms up to $\mathcal{O}(r^{-2})$ and $\mathcal{O}(r^{-4}\log(r))$ (and analogously for S and A). When using spectral methods, it is especially important to subtract a high number of logarithmic NB terms, as spectral methods rely on regularity of the functions presented. Lastly, it is convenient to apply a gauge transformation $r \to r + \xi(t)$ such that the apparent horizon (AH) remains at a constant value of the r coordinate. Since the condition for the location of the AH equals $\dot{S} = 0$ the equation for $\xi(t)$ can be obtained by solving $\partial_t\dot{S} = 0$ on the AH (note that in Fig. 5 of the main text we do not apply this gauge transformation for clarity).

The methods to couple the equations with our boundary Friedmann+inflaton equations are exactly the same as in [9] with the only exception that we now have a dynamical source for the scalar field as is detailed in the main text. For completeness we note that we use a pseudospectral grid with 5 domains each having 7 grid points. In the simulations we use $\kappa_5 = 1$ and rescale to the chosen κ_5 only when plotting results. We use timesteps of $\delta t = 0.0005$ and filter then numerical functions every 50 timesteps by interpolating back and forth to a spectral grid with 5 points (see also [13]). We start with a radial gauge transformation $r \to r + \xi$ with $\xi = 1.709$. This fixes the apparent horizon at $z = 1/r = 0.36$ and the evolution equations for $\xi(t)$ guarantee that the horizon stays there (nevertheless, every 100 timesteps we perform a tiny gauge transformation to bring it back to $z = 0.36$). The full evolution then takes around 200 hours on a single core using *Mathematica* 11.

For reference we note that the temperature as derived from the surface gravity κ can be obtained from $T_{\mathrm{AH}} = \kappa/2\pi = -\frac{z^2}{4\pi}\partial_z A$ evaluated at the location of the apparent horizon. For the event horizon this requires solving the differential equation $\partial_t r_{\mathrm{EH}} = -\frac{1}{2}A$ with boundary condition $A(t, r_{\mathrm{EH}}(t = \infty)) = 0$. This reflects the fact that the event horizon is teleological, e.g. it depends on the future spacetime. In our simulations we go to a finite time where the geometry is sufficiently constant such that a full solution of the event horizon can be obtained.

The full code can be downloaded at wilkevanderschee.nl.

[1] G. Compere and D. Marolf, Class. Quant. Grav. **25**, 195014 (2008), arXiv:0805.1902 [hep-th].

[2] A. Ishibashi, K. Maeda, and T. Okamura, (2023), arXiv:2301.12170 [hep-th].

[3] Y. Ahn, M. Baggioli, K.-B. Huh, H.-S. Jeong, K.-Y. Kim, and Y.-W. Sun, JHEP **02**, 012 (2023), arXiv:2211.01760 [hep-th].

[4] M. Bianchi, D. Z. Freedman, and K. Skenderis, JHEP **08**, 041 (2001), arXiv:hep-th/0105276.

[5] M. Bianchi, D. Z. Freedman, and K. Skenderis, Nucl. Phys. B **631**, 159 (2002), arXiv:hep-th/0112119.

[6] K. Skenderis, Class. Quant. Grav. **19**, 5849 (2002), arXiv:hep-th/0209067.

[7] M. Henningson and K. Skenderis, JHEP **07**, 023 (1998), arXiv:hep-th/9806087.

[8] I. Papadimitriou, JHEP **08**, 119 (2011), arXiv:1106.4826 [hep-th].

[9] C. Ecker, W. van der Schee, D. Mateos, and J. Casalderrey-Solana, JHEP **03**, 137 (2022), arXiv:2109.10355 [hep-th].

[10] J. Casalderrey-Solana, C. Ecker, D. Mateos, and W. Van Der Schee, JHEP **03**, 181 (2021), arXiv:2011.08194 [hep-th].

[11] M. Attems, J. Casalderrey-Solana, D. Mateos, I. Papadimitriou, D. Santos-Oliván, C. F. Sopuerta, M. Triana, and M. Zilhão, JHEP **10**, 155 (2016), arXiv:1603.01254 [hep-th].

[12] P. M. Chesler and L. G. Yaffe, Phys. Rev. Lett. **102**, 211601 (2009), arXiv:0812.2053 [hep-th].

[13] P. M. Chesler and L. G. Yaffe, JHEP **07**, 086 (2014), arXiv:1309.1439 [hep-th].

[14] W. van der Schee, *Gravitational collisions and the quark-gluon plasma*, Ph.D. thesis, Utrecht U. (2014), arXiv:1407.1849 [hep-th].